UNIVERSITÀ
DEGLI STUDI
DI PADOVA

Head Office: Università degli Studi di Padova

Department of Molecular Medicine

Ph.D. COURSE IN: MOLECULAR MEDICINE
CURRICULUM: REGENERATIVE MEDICINE
SERIES 35TH

Decellularized Human Diaphragm Muscle as a Biologic Scaffold for Reconstructive Surgery

Coordinator: Ch.mo Prof. Riccardo Manganelli
Supervisor: Ch.mo Prof. Prof. Vincenzo Vindigni

Ph.D. student: Dott. Federico Facchin

INDEX

ABSTRACT

Therapeutic options available in the clinical practice to restore severe loss of muscle mass after trauma or tumor excision offer limited functional and aesthetic results and they are limited by several drawbacks, such as donor site morbidities and increased risk of complication.

Thus, tissue engineering is focusing on the development of alternative strategies to induce and favor tissue regeneration limiting scar formation and fibrosis. Among those, the creation of 3-D scaffold has shown favorable results thanks to its tissue-specificity and ability to stimulate cell differentiation toward the tissue of origin.

In this project, we aimed to create a decellularized human-derived scaffold from diaphragm muscle. Four different detergent-enzymatic protocols were compared to identify the ideal treatment to remove immunogenic signals maintaining structural and functional properties to allow scaffold implantation and cell seeding. Together with DNase I and Trypsin, four different detergents (sodium dodecyl sulfate, SDS + Tergitol^{TM}, sodium deoxycholate and Tergitol^{TM}) were compared.

All protocols were able to remove nuclei, DNA and muscle fibers preserving collagen, elastin and glycosaminoglycans. In addition while HLA-DR was no more detectable, Collagen I and IV, Laminin (key components of the ECM) were expressed. Macroscopic evaluation and tensile strength confirmed the preservation of functionality and structure without differences among protocols.

Adipose-derived mesenchymal stem cells co-culture and seeding showed absence of cytotoxicity and ability of the graft to support cell proliferation after all decellularization.

Protocol n. 2 (SDS + Tergitol^{TM}) exhibited the higher preservation of collagen structure and fibers orientation. For this reason scaffolds treated with this protocol were implanted in mice for 14 days during the in vivo biocompatibility test, which demonstrated favorable integration with VEGF positivity and without signs of severe immunological response from the host.

INTRODUCTION

Reconstruction of extensive area of the body represents the constant challenge of plastic surgeons influencing the patient's quality of life and preventing the normal performance of daily activities.

Nowadays, the concept of reconstructive ladder has been outdated by the reconstructive elevator and clockwork [1].

Autologous-based flap reconstruction is considered the gold standard reconstructive method in main area of the body [2]. However, it is affected by donor site morbidity. In addition, not all reconstructive options are available or adequate such as in case of previous surgeries or failure of previous autologous reconstruction. Acellular dermal matrixes (ADMs) are proposed to restore dermal layers after extensive tissue loss as in abdominal wall reconstruction and breast reconstruction [3,4].

Volumetric muscle loss (VML), a condition characterized by the loss of at least 20% of a given muscle [5]. It can be developed after severe trauma, such as car accidents, battle wounds or tumour excision [6-8], and it is associated with significant functional impairment and aesthetic damage [9].

The alteration of the quality of life with the impairment of daily activities and rehabilitation affects patient's recovery [10,11]. Corona et al. reported that VML contributed 65 percent to the permanent disability in the type III open tibia fracture cohort [12].

Even though skeletal muscle presents a high regenerative potential thanks to its reservoir of muscle satellite stem cells (MuSCs), aforementioned conditions can cause damages that overcome its ability to regenerate, in particular when the extracellular matrix (ECM) is compromised extensively [13].

Available clinical treatment options are aimed in the optimization of the remaining functional activity after injury, but there are currently no therapies available to regenerate these extensive soft-tissue injuries to restore original form and

function. In fact, rehabilitative protocol showed limited benefit. While surgical approach offers inadequate restoration of muscle function and persistence of limb functioning deficit frequently aimed only in wound/bone coverage with autologous local or free tissue transfer after debridement.

Autologous free functional muscle transfers to the extremities have shown good results in terms of function restoration with several different donor-site options (i.e. gracilis, latissimus dorsi, rectus femoris, and vastus lateralis). However, surgical complications such as donor site morbidity, infection and failure of reconstruction must be considered [14-19].

For these reasons, alternative therapies are needed to restore the loss of volume of skeletal muscle tissue, possibly stimulating its regeneration for functional recover.

Tissue Engineering (TE) has been proposed to support and induce muscle regeneration. Traditionally, the triad including progenitor cells, scaffold and growth factors has been considered the pillars of tissue regeneration. Different types of scaffold have been developed to support cell growth and cultures. In vitro formation of muscle graft has shown limitations due to its easy degradation, risk of foreign body response and functional deficits. In addition, a parallel disposition of muscle fibers, vascularization and innervation are needed to form functional skeletal muscles [20,21].

On the other hand, biological scaffolds derived from decellularized tissue that maintain the original ECM structure have been suggested to promote cell differentiation in myogenic progenitors or inducing the recruitment of tissue resident or circulating progenitor cells in situ [5,22-24].

The first decellularization protocol was developed by Carlson and Carlson in 1991, who proposed a method involving several steps based on chelants, detergent and enzymatic digestion with DNAse [25]. Subsequently, the role of physical treatment, additional enzymatic reaction, and chemicals was confirmed, thus protocols based on a combination of these different methods were preferred [26]. The process usually

starts with lysis of the cell membrane induced by physical treatments or ionic solutions, then cells are separated from ECM with enzymatic treatments, and detergents are used to solubilize cytoplasmic and nuclear content. Lavages and final removal of cellular debris is performed. Mechanical agitation can be used to increase their effectiveness [27].

The majority of allogenic and xenogenic matrixes developed and available in the clinical settings are derived from thin tissues such as dermis, bladder and mucosa (e.g. human dermis = Alloderms®, porcine dermis = Braxon®/Strattice®, SurgiMend® = bovine dermis, porcine SIS = SurgiSISs®, porcine urinary bladder = ACell, porcine heart valves = Synergrafts®) [28-31].

Muscle-derived xenogenic scaffolds have been studied in preclinical studies in mouse, rat, rabbit, pig and dog in animal models of wound treatment, muscle reconstruction and VML. They have been shown to improve muscle regeneration in animal models alone and in association with stem cells [6,13,30]. Main components of muscle ECM (laminin, fibronectin, collagens, proteoglycans) together with growth factors were able to recruit muscle progenitors cells guiding the differentiation in myoblast muscle fiber [32-34].

However, biologic scaffold materials of xenogenic origin may elicit a stronger foreign-body reaction when implanted. On the other hand, scaffold derived from human skeletal muscle has not been extensively investigated [35].

Thanks to its anatomy, availability and structure human diaphragm can be considered a valid option for human muscle restoration. Favorable results were obtained with orthotopic diaphragm reconstruction with animal derived scaffold in mice, rats, bovines and pigs [36-41].

In addition, the same scaffold was applied for the treatment of chronic wounds and abdominal wall defects animal models [42,43]. A limited number of reports regarding human-diaphragm decellularization protocol are available in the literature [44].

1.1 AIM OF THE STUDY

The project aimed in developing a valid decellularization protocol of human diaphragm. In vitro characterization of tissue samples was performed analyzing immunogenicity, ECM preservation and tissue properties. In addition, scaffold biocompatibility was verified in vivo.

MATERIALS AND METHODS [45]

2.1 SAMPLES COLLECTION

Six human diaphragms were collected from healthy cadaver donors from the Body Donation Program of the Section of Human Anatomy, University of Padova, according to national and international body donation protocols [46,47].

2.5 × 2.5 cm^2 patches were prepared and frozen at −20 ◦C. Figure 1

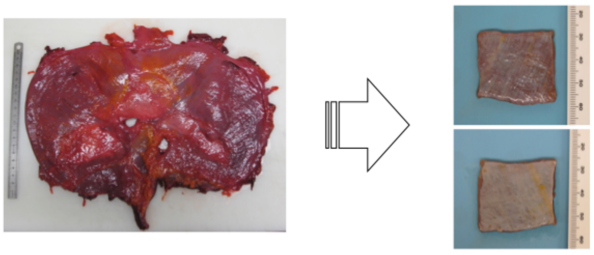

Diaphragmatic skeletal muscle from human cadaver

2.5x2.5mm^2 Patches for decellularization

2.2 DECELLULARIZATION OF HUMAN DIAPHRAGMATIC MUSCLE

Tissue samples were handled under sterile condition. Removal of tissue contaminants, debridement and washing with antibiotic and PBS were performed. Four detergent-enzymatic protocols were tested. All of them required less then six days to be completed. Table 1

	Protocol n. 1	Protocol n. 2	Protocol n. 3	Protocol n. 4
Process	**dH_2O** (24 h at 4°C) **DNase in NaCl 1M** (3h, at room temperature) **0.05% Trypsin + 0.02% EDTA in PBS** (1 h at 37 °C) **0.5% SDS + 0.8% NH_4OH in PBS** (72 h at 4 °C) **dH_2O** (48 h at 4 °C)	**dH_2O** (24 h at 4°C) **DNase in NaCl 1M** (3h, at room temperature) **0.05% Trypsin + 0.02% EDTA in PBS** (1 h at 37 °C) **0.5% SDS + 0.8% NH_4OH in PBS** (48 h at 4 °C) **0.5% Tergitol™ + 0.8% NH_4OH in PBS** (24 h at 4 °C) **dH_2O** (48 h at 4 °C)	**dH_2O** (24 h at 4°C) **DNase in NaCl 1M** (3h, at room temperature) **0.05% Trypsin + 0.02% EDTA in PBS** (1 h at 37 °C) **4% SDC + 0.8% NH_4OH in PBS** (72 h at 4 °C) **dH_2O** (48 h at 4 °C)	**dH_2O** (24 h at 4°C) **DNase in NaCl 1M** (3h, at room temperature) **0.05% Trypsin + 0.02% EDTA in PBS** (1 h at 37 °C) **0.5% Tergitol™ + 0.8% NH_4OH in PBS** (72 h at 4 °C) **dH_2O** (48 h at 4 °C)
N. of cycles	1	1	1	1

2.3 CHARACTERIZATION OF DECELLULARIZED DIAPHRAGMATIC PATCHES

2.3.1 Histological Investigations

All samples were fixed with 10% formalin, paraffin-embedded and cut into 5 μm sections, which were de-waxed and rehydrated with cycles in ethanol (99%, 95% and 70%) and distilled water. Histological staining was performed in order to evaluate cell nuclei, muscle fibers (Hematoxylin&Eosin), myofibrillar component and collagen (Azan-Mallory), elastic fibers (Weigert Van Gieson) and collagen (Masson's trichrome).

2.3.2 Immunohistochemical Study

Anti-Collagen I (polyclonal rabbit anti-COL1A1, sc-28657, Santa Cruz Biotechnology, Dallas, TX, USA) (1:500), anti-Collagen IV (monoclonal mouse anti-COL4A3, sc-52317, Santa Cruz Biotechnology) (1:100), anti-Laminin (polyclonal rabbit anti-LAM, L9393, Merck Life Science) (1:200), anti-HLA-DR (monoclonal mouse anti-HLA- DR antigens, M0746, Dako) (1:50) antibodies were used to evaluate the preservation of ECM proteins and removal of immunologic signals after decellularization protocols.

Immunohistochemical reactions were carried out with Dako Autostainer/Autostainer Plus (Dako, Milan, Italy) using antibodies diluted in PBS both in native and decellularized samples. Epitope retrieval was performed with 10 mM of sodium citrate buffer at 90°C for ten minutes at pH 6.0 for Collagen I and HLA-DR and pH 9.0 for Collagen IV. Five minutes incubation with peroxidase-blocking serum (EnVision FLEX Peroxidase-Blocking Reagent; Dako) was performed to prevent unspecific binding before one-hour incubation of primary antibody at room temperature.

Secondary antibodies (EnVision FLEX Mouse-Linker and EnVision FLEX Rabbit- Linker; Dako) were then incubated for 15 minutes followed by EnVision FLEX/HRP polymer for 20 min. Positive reaction was highlighted with 3,3′-

diaminobenzidine (EnVision FLEX Substrate Buffer + DAB + Chromogen; Dako). Sections were then counterstained with haematoxylin.

2.3.3 Morphometric Analysis

The content of connective tissue was quantified with Image J as percentage of color areas on Azan-Mallory-stained (blue collagen) and Weigert Van Gieson-stained (purplish elastin) sections and compared between treated and native samples. Pictures were taken considering 8 different fields/section for each experimental group and they were acquired at 10x magnification in bright field with Image J [48-50].

The colors of each picture were analyzed, displaying histograms of the distribution of hue, saturation and brightness. The interval of hue, saturation and brightness of blue (128–200, 0–255, and 0–224) and purplish (127–225, 0–255, and 0–185) areas was selected manually and maintained for all the morphometric analyses.

The selected interval of colors was converted into black and all other colors into white. To facilitate the process of evaluation, the white and black colors were inverted. On the processed images, the white areas corresponding to collagen and elastic fibers elaborated from Azan-Mallory-stained sections and Weigert Van Gieson-stained sections respectively, were measured as percentage of area stained out of the total acquisition field.

2.3.4 Quantification of residual DNA

Evaluation of DNA remnants after each protocol was performed as a measure of ability to remove immunogenic materials of cells and nuclei. The DNeasy Blood and Tissue Kit was used. Proteinase K (Merck Life Science) was used to lysate 10 mg of sample at 56 °C overnight. DNeasy Mini spin columns allowed selective purification of total DNA from lysates. Fluorometric quantification of DNA was

obtained with Qubit 4 fluorometer and kit (ThermoFisher Scientific, Waltham, MA, USA).

2.3.5 Glycosaminoglycans Quantification

Chondrex Inc. Glycosaminoglycans Assay Kit (DBA Italia S.r.l., Milan, Italy) was used to quantify residual GAGs based on GAG solubilization and dimethylmethylene blue (DMB) colorimetric reaction. Papain solution at 56°C overnight was used for the digestion of 10 mg of tissue sample (10 mg) and GAGs solubilization. The cationic dye 1,9 dimethylmethylene blue (DMB) was used to label solubilized GAGs and colorimetric reaction was read at 530 nm by using the Microplate auto reader VICTOR3TM (PerkinElmer, Waltham, MA, USA). Results were compared between decellularized and native samples.

2.4 Second Harmonic Generation Microscopy

Second Harmonic Generation (SHG) imaging was performed on paraffin embedded samples to define and compare the amount and the orientation of collagen fibers.

An incident wavelength of 800 nm was adopted to detect the collagen's SHG signal at 400 nm and the AutoF signal at 525 nm on two different photodetectors (GaAsP PMT with 395/25 nm bandpass filter and GaAsP PMT with 525/40 nm bandpass filter, respectively). Image-J software was used to analyze 70 consecutive frames, with a pixel dwell time of 0.14 µs and a pixel width of 0.8 µm obtained with a water immersion objective Olympus 25X with 1.05 numerical aperture (1024 × 1024 pixels).

Coherency (C), a parameter indicating the presence (value 1 = anisotropy) or absence (value 0 = isotropy) of a dominant orientation of collagen and elstic fiber, was estimated with OrientationJ, an ImageJ plugin.

The Fast Fourier Transform (FFT) analysis of the coherency allowed a specific representation of fibers orientation: highly oriented fiber in a single direction shows an elliptic shape; differently, a circular shape is associated to fibers spread in all directions [51-54].

2.5 TENSILE TESTING

Rectangles of 5 mm x 15 mm both longitudinal and transverse to muscle fibers were prepared (i.e. 3 per each group). Bose ElectroForce® Planar Biaxial Test Bench instrument was used to evaluate the stress response to five cycles of 22N strain. Strain (a measure of tissue stiffness) was defined by the ratio between displacement and initial length Stress was calculated as the ratio between the force applied and the initial transverse area of the sample. The secant elastic module was calculated as the slope of the straight line drawn from the origin of the stress-strain and intersecting experimental data at 20% of strain during the fifth cycle [55].

2.6 IN VITRO CYTOTOXICITY

Indirect co-culture test was performed to evaluate a possible persistence of cytotoxic molecules after decellularization processes.

Discoidal samples of diaphragm (8 x 2 mm) were sterilized with 72 h incubation of 2% penicillin/streptomycin solution (Merck Life Science). Subsequent sterile water washing was performed for 72 h to remove antibiotic.

24-well plates (5000 cells/cm2) of proliferating human adipose-derive mesenchymal stem cells (Ad-MSCs) (Cell Line Service, Eppelheim, Germany) on Mesenchymal Stem Cells Expansion Medium (Cellular Engineering Technologies, Coralville, IA, USA) + 10% Foetal Bovine Serum (Merck Life Science) and 1% penicillin/streptomycin solution (Merck Life Science) were co-cultured with previously sterilized samples by mean of a porous membrane with 8 μm pore size for 72 h at

37°C and 95% of humidity. The co-culture with native sample was the negative control while Ad-MSCs cultures with 50% DMSO were used as positive control.

Cell viability was confirmed with MTT assay. Cultured cells were incubated with 0.5 mg/ml of 3-(4,5-dimethylthiazol-2-yl)-2,5-diphenyltetrazolium bromide for 4 hours. The formazan formed was solubilized with 0.04 M HCl in 2-propanol and the optical density was calculated with the Microplate auto reader with a 570 nm wave light. The percentage of metabolically active cells in samples compared to native diaphragm was calculated.

2.7 Cell Seeding on Acellular Diaphragmatic Scaffold

Ad-MSCs were seeded in sterilized diaphragm patches to evaluate the ability of cell to proliferate and adhere on treated scaffold. 4 mm discoidal samples of diaphragm were sterilized with 72 h incubation of 2% penicillin/streptomycin solution (Merck Life Science). Subsequent sterile water washing was performed for 72 h to remove antibiotic. A culture in basal medium with 10% fetal bovine serum at 37 °C, 5% CO^2 and 95% humidity was used to perform a microbiologic test and to select diaphragmatic disks free from microbiological contamination (fungal or bacterial).

The selected disks placed over a 96-well plate were treated with Ad-MSC proliferation medium at 37 °C overnight and then they were seeded with 10,000 Ad-MSCs/scaffold in 200 µL of proliferation medium for 7 days.

Subsequently, MTT assay was used to evaluate cell viability: the number of cell detected on scaffold was used to create an MTT standard curve. Different number of Ad-MSCs per well (1000, 5000, 10,000, 20,000, and 100,000) were seeded in 96-well plates and let adhere for 12 h. The MTT assay was used to calculate cell viability with different number of cells per well obtaining different optical density values corresponding to different point of the curve. Optical density values measured for each sample were plotted on the standard curve to quantify cell growth on seeded scaffolds.

In addition, tissue samples with cultured cells were fixed with 2.5% glutaraldehyde in 0.2 M phosphate buffer, washed, dehydrated and coated with 8 nm gold layer for ultrastructural evaluation with tungsten thermionic emission SEM system JSM-6490 to analyze the superficial ultrastructure of cultured cells.

2.8. IN VIVO BIOCOMPATIBILITY

8 x 2 mm sections of decellularized diaphragm treated with Protocol n. 2 were sterilized and implanted subcutaneously in the dorsum of six twelve years old female mice. The patches were sutured to the latissimus dorsi (LD) muscle and the skin was closed. Antibiotic and anti-inflammatory therapies were administered for the first 5 days and the animals were sacrificed after 14 days.

Macroscopic and microscopic (histologic, immunohistochemical, scanning microscopy) analyses were performed. In addition to standard haematoxylin and eosin staining, antibodies anti- CD3 (polyclonal rabbit anti-CD3, A0452, Dako) (1:500) and anti-F4/80 (polyclonal rabbit anti-F4/80 (M-17)-R, sc-26643-R, Santa Cruz Biotechnology) (1:1000) were used to evaluate the amount and the localization of lymphocytes and monocytes/macrophages, respectively. Furthermore, anti-VEGF antibodies (monoclonal mouse anti-VEGF, C-1, sc-7269, Santa Cruz Biotechnology) (1:300) and anti-myosin antibody (monoclonal mouse anti-slow muscle myosin, MAB1628, Merck) (1:1500) were used to evaluate the amount of angiogenic infiltration and myogenic stimulation. Secondary antibodies and diaminobenzidine were used to detect a positive reaction.

2.9. STATISTICAL ANALYSIS

Data are presented as mean ± standard deviation (SD) of at least three replicates. The ANOVA test followed by the Tukey post-hoc test for multiple comparisons were used for statistical significance ($p \leq 0.05$).

RESULTS

3.1 DIAPHRAGM DECELLULARIZATION

After decellularization with all four detergent-enzymatic protocols human samples maintained a volume and a 3-D structure similar to the native sample without macroscopically visible tears or ruptures. Figure 2

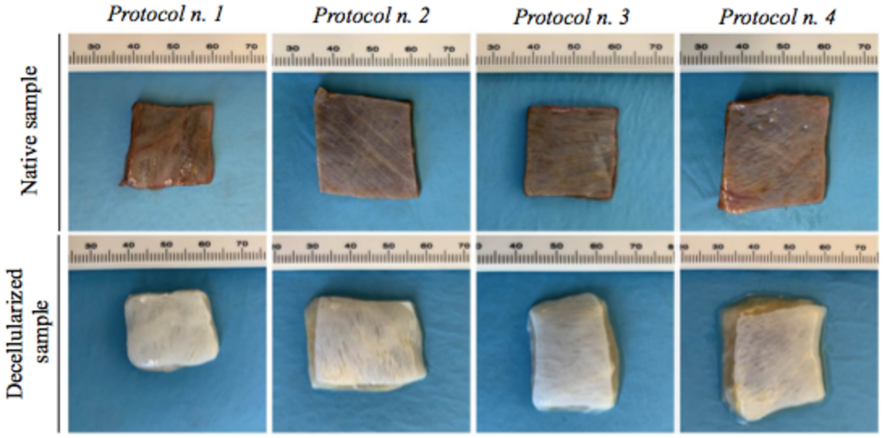

Figure 2. Macroscopic aspect of diaphragmatic samples before and after decellularization

A lighter color was noted for each samples compared to native tissue. Samples treated with Protocol n. 4 showed a reduced compactness and manipulability.

3.2. HISTOLOGICAL AND IMMUNOHISTOCHEMICAL INVESTIGATION

Haematoxylin and eosin staining displayed the elimination of cells, nuclei and muscle fibers from the treated samples and the preservation of the 3D structure of the ECM. Figure 3

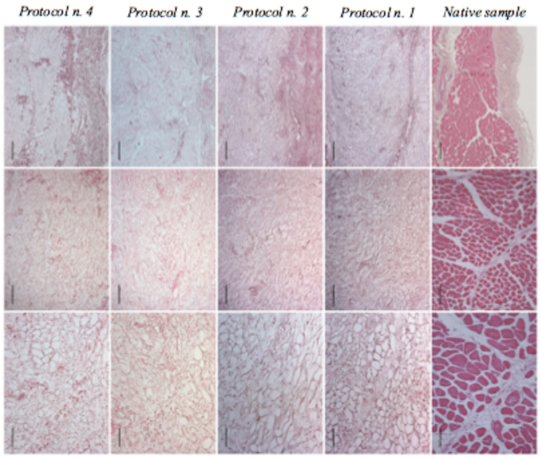

Figure 3. Haematoxylin and eosin staining showing elimination of cells, nuclei and muscle fibers and preservation of 3D structure of the ECM.

Azan-Mallory, Weigert Van Gieson, and Masson's trichrome staining allowed to recognize the preservation of collagen, elastic fibers and vessel structures. On the contrary, muscle fibers appear to be clearly removed. Figure 4

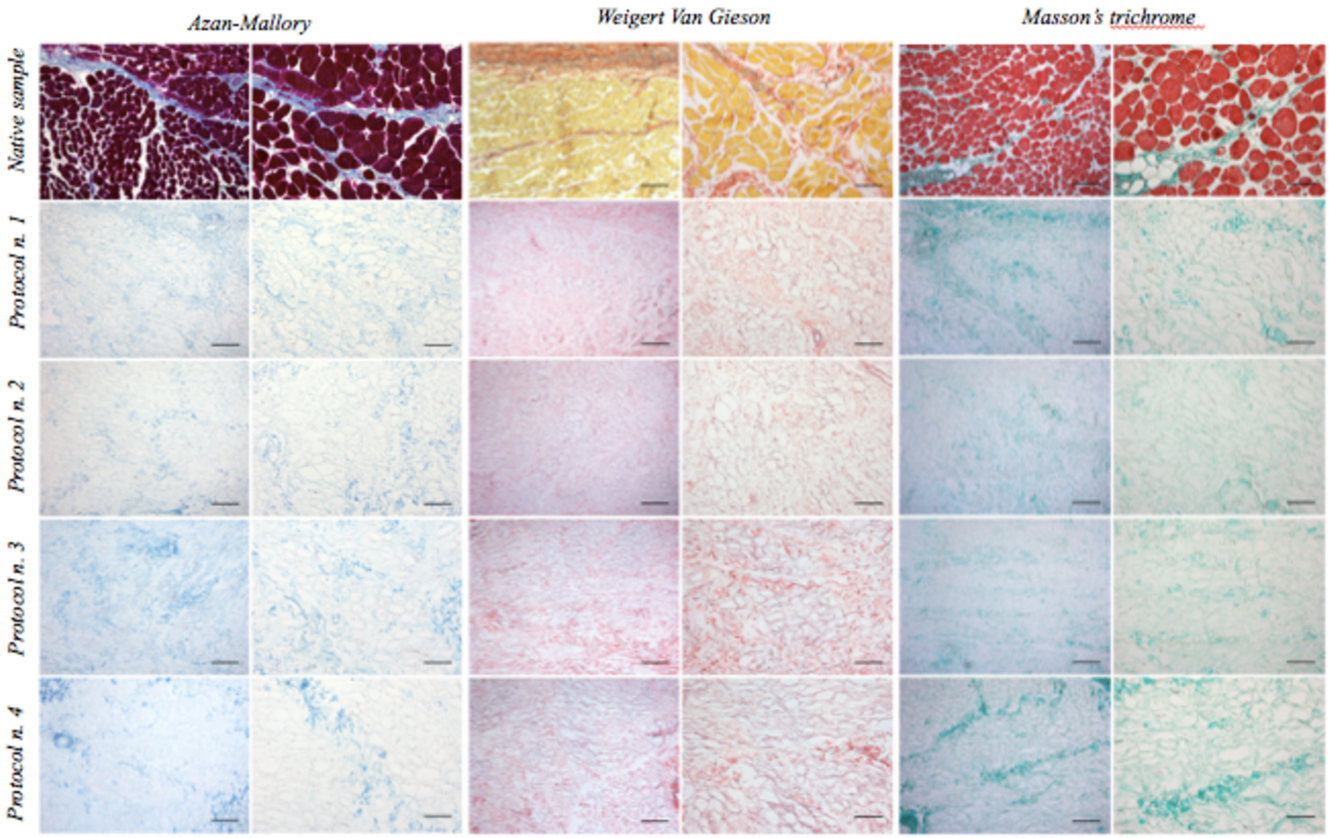

Figure 4. Azan-Mallory, Weigert Van Gieson, and Masson's trichrome stainings showed nuclei and muscle fibers removal and the preservation of ECM structures and protein (i.e. Collagen and elastic fibers).

Immunoistochemical investigation confirmed the preservation of Collagen I, Collagen IV and Laminin. In particular, the basement membrane between endomysium and muscle fiber sarcolemma was preserved in treated samples. A reduced reaction to Collagen I and Laminin was appreciated after Protocol n. 4. Figure 5

The positivity to HLA-DR antigens at cellular level of the native samples was absent after the treatment with each protocol.

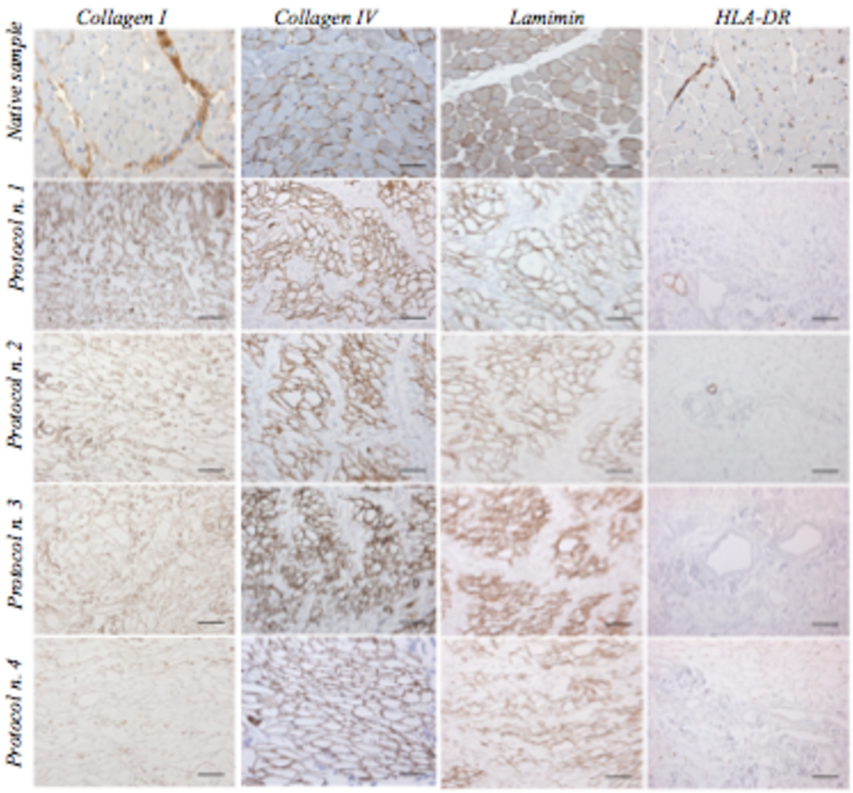

Figure 5. Collagen I, Collagen IV, Laminin immunolocalization showed the preservation of ECM structures. The removal of HLA-DR showed an efficient removal of immunogenic molecules from treated samples.

3.3. QUANTITATIVE ANALYSES

The DNA content was below the threshold level stated in the literature (50 ng/mg) in all treated samples [56,57]. Figure 6A

The percentage of color areas on Azan-Mallory-stained (blue collagen) and Weigert Van Gieson-stained (purplish elastin) sections showed similar value without statistically significant differences between native and treated samples. Figure 6B,C

As for GAGs quantification, all protocols determined a comparable reduction of the GAG content after treatment, without a statistically significant difference between different protocols, with a 60-70% of GAG preservation compared to the control group, with slightly higher preservation after the treatment with protocol n. 4. Figure 6D.

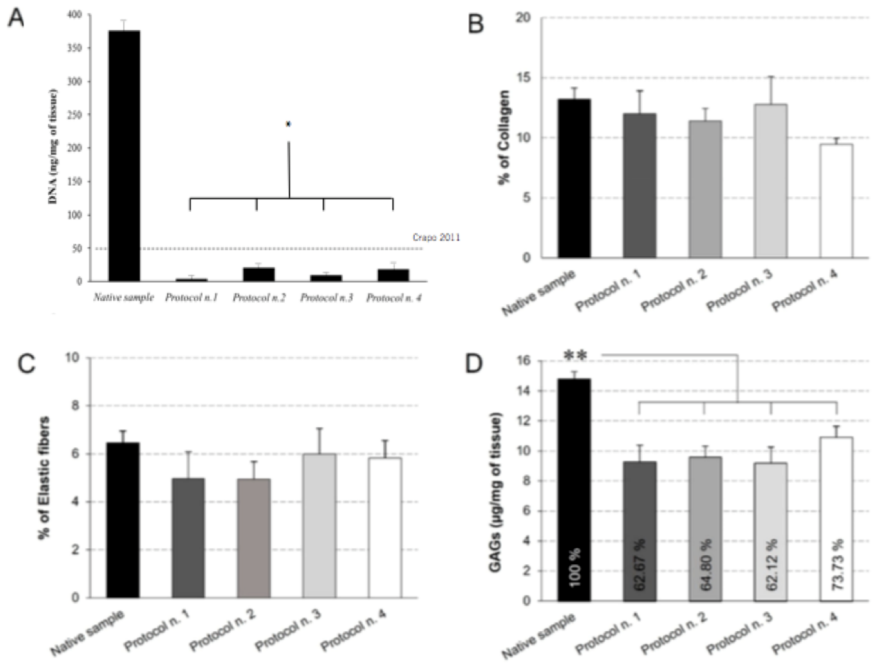

Figure 6. Quantification of **A** residual DNA, **B** Collagen, **C** elastic fibers, **D** GAGs. From Barbon S, Stocco E, Contran M, Facchin F, Boscolo-Berto R, Todros S, Sandrin D, Romanato F, Pavan P, Macchi V, Vindigni V, Bassetto F, De Caro R, Porzionato A. Preclinical Development of Bioengineered Allografts Derived from Decellularized Human Diaphragm. Biomedicines. 2022 Mar 22;10(4):739.

3.4. SHG IMAGING

The mean intensity of the signal obtained was comparable between each treated sample and native tissue, confirming the preservation of collagen fibers after each treatment. Fast Fourier Transform (FFT) analysis (a graphic representation of the coherency), together with coherency values, showed a different behavior between treated and native samples. In fact, in the native samples the collage fibers appeared to be oriented in an ordinate single direction.

On the contrary, the collagen in the majority of decellularized samples lost the ordinate disposition, except for tissues treated with Protocol n. 2, which maintained original orientation of collagen fibers with significant differences compared to other samples. Figure 7, 8

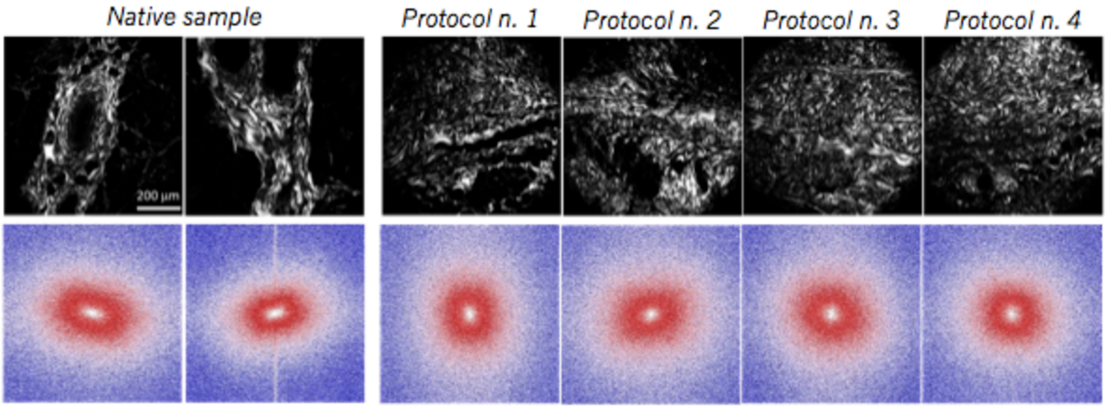

Figure 7. SHG collagen analysis (**above**) and Fast Fourier Transforms – FFTs (**below**) showing an ellipsoidal orientation of fibers typical of anisotropic behavior in native samples vs. a spherical fiber orientation decellularized samples

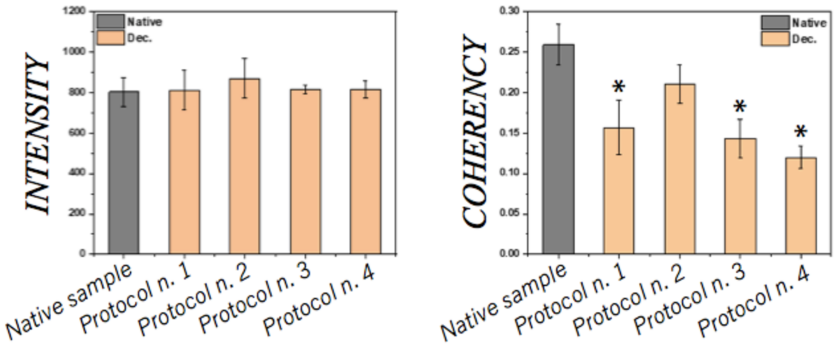

Figure 8. No significant differences in the intensity of the collagen signal (**Left**). Coherency (**Right**), a collagen fibers orientation estimate showed significant impact on the orientation of the fibers from all protocols except Protocol n. 2

3.5. STRESS–STRAIN RESPONSE

According to the classic response of dissected tissues, which need initial preconditioning, the stress value decreased significantly (almost 15% for the first two cycles) during initial cycles. Only in last cycles of stimulation the stress response to the strain was consistent.

During the fifth cycle samples developed a nonlinear response to strain with exponential increase in the stress response and an increase of the strain in all samples. Samples treated with Protocol n. 4 were the stiffest. Figure 9 A–H

Only native samples showed a different stress-strain response according to the direction of the strain, with lower stress after a strain longitudinal to muscle fibers (anisotropy) [58].

The secant elastic module allowed to recognize statistically significant difference in stiffness level between all protocols both in longitudinal and transverse direction (p=0.022-0.009 respectively). All treated samples developed an isotropic behavior except for Protocol n. 4. Figure 9 I–K

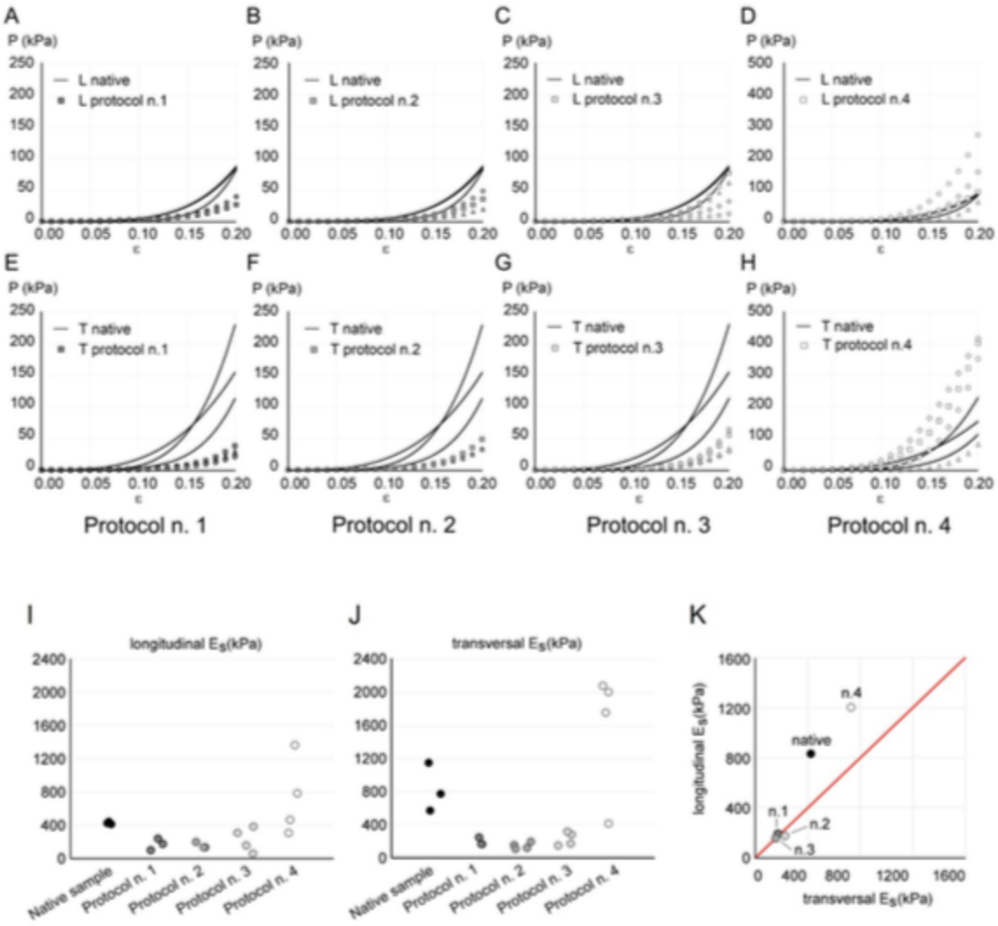

Figure 9. Comparison of the stress response to a longitudinal (**A to D**) and trasversal (**E to H**) strain between native samples and samples treated by each protocol. Given to the higher stiffness the y axe of graphs D and H have different values. Longitudinal (**I**) and transversal (**J**) secant elastic modules used to compare each protocol. Mean values of longitudinal and transversal secant elastic modules used to evaluate the isotropy of the response (=equal response to strain vs. anisotropy typical of native tissue). From Barbon S, Stocco E, Contran M, Facchin F, Boscolo-Berto R, Todros S, Sandrin D, Romanato F, Pavan P, Macchi V, Vindigni V, Bassetto F, De Caro R, Porzionato A. Preclinical Development of Bioengineered Allografts Derived from Decellularized Human Diaphragm. Biomedicines. 2022 Mar 22;10(4):739.

3.6. CYTOCOMPATIBILITY STUDIES

A preservation of Ad-MSCs viability higher than 80%, without statistically significant differences among protocols, was highlighted by the 72 hours indirect co-culture test. Figure 10A

Similarly, the MTT assay of cells cultured on treated diaphragm samples showed the presence of viable and proliferative cells without difference among different protocols. Figure 10B

A normal layer of proliferating cells was recognizable on all scaffolds. Figure 10C

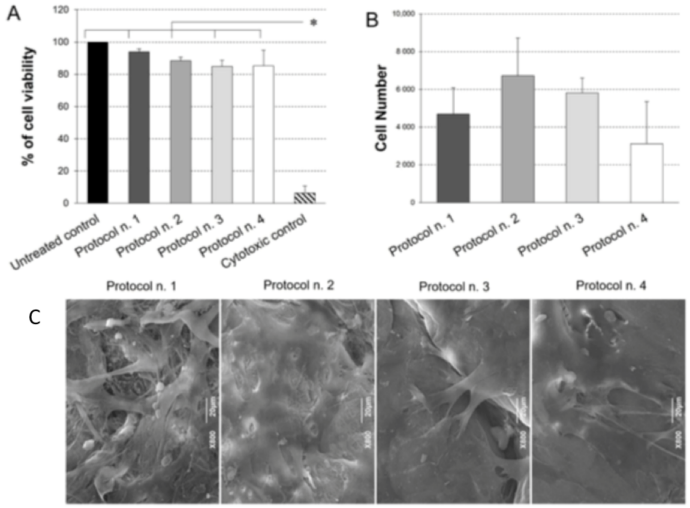

Figure 10. Ad-MSCs viability after 72 h of indirect co-culture >80% in decellularized scaffold vs. DMSO cytotoxic control evaluated with MTT assay (**A**). Ad-MSCs growth and proliferation after 7 days of culture evaluating the number of cells detected with MTT assay (**B**). Surface morphology of scaffolds after cultures: adherent monolayer of cells in SEM microscopy (**C**). From Barbon S, Stocco E, Contran M, Facchin F, Boscolo-Berto R, Todros S, Sandrin D, Romanato F, Pavan P, Macchi V, Vindigni V, Bassetto F, De Caro R, Porzionato A. Preclinical Development of Bioengineered Allografts Derived from Decellularized Human Diaphragm. Biomedicines. 2022 Mar 22;10(4):739.

3.7. IN VIVO BIOCOMPATIBILITY STUDY

Fourteen days after implantation, the samples treated with Protocol n. 2 developed a mild capsule without signs of reabsorption or severe reaction. Histological evaluation displayed signs of integration with limited cells response at the superficial and deep interface between the scaffold and the host. SEM images confirmed preservation of collagen fibers without massive cell invasion.

Mild CD3 and F4/80 positivity was localized at the contact surface between the graft and the host without signs of severe invasion. VEGF positivity was detected in the graft. On the contrary, no myosin positivity was detected. Figure 11

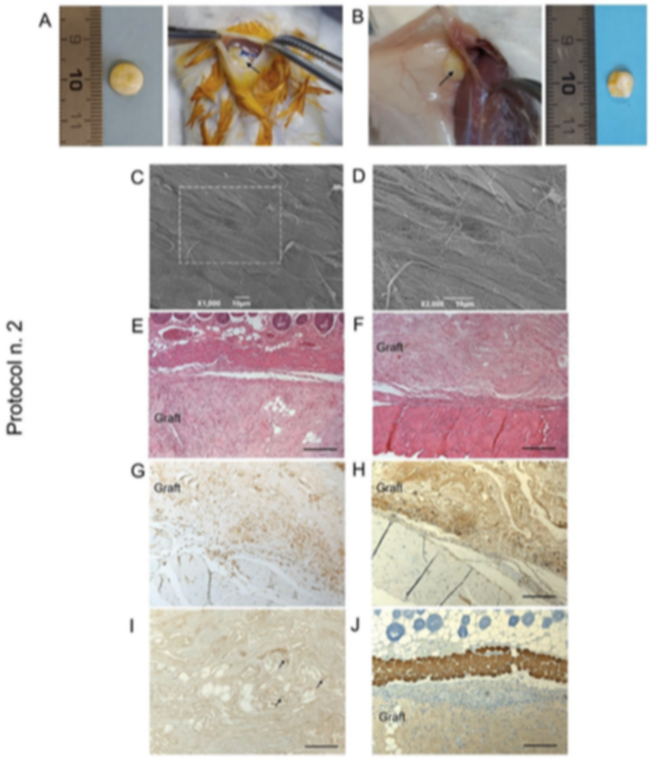

Figure 11. Evaluation of in vivo biocompatibility of scaffold decellularized with Protocol n. 2. (**A**) Implantation of 8 x 2 mm of sample anchored to the LD muscle from a dorsal subcutaneous incision. (**B**) Explantation after 14 days and macroscopic evaluation without signs of infection or reaction. Evaluation of ultrastructural (**C** = superficial, **D** = deep) and histological (**E** = superficial, **F** = deep) analysis showing preserved collagen organization and absence of lympho-monocytic invasion in both contact surface between scaffold and host. Moderate immunologic response with location of CD3+ (**G**) and F4/80+ (**H**) cells at graft borders. VEGF+ location in the sample (**I**) showing early angiogenic process but limited myogenic response (**J**). Scale bar: 10 µm (**C**,**D**); 200 µm (**E**–**J**). From Barbon S, Stocco E, Contran M, Facchin F, Boscolo-Berto R, Todros S, Sandrin D, Romanato F, Pavan P, Macchi V, Vindigni V, Bassetto F, De Caro R, Porzionato A. Preclinical Development of Bioengineered Allografts Derived from Decellularized Human Diaphragm. Biomedicines. 2022 Mar 22;10(4):739.

DISCUSSION

The triad of tissue engineering (i.e. cells cultures, scaffolds and growth factors) is a concept commonly used to describe the strategies available in regenerative medicine. The importance of scaffolds and extracellular matrix (ECM) is well known: they not only act as structural support for cell attachment, growth, migration and proliferation but also induce tissue-specific differentiation. In fact, the ECM provides bioactive signals for cell regulation and it is a reservoir of growth factor itself [59-62].

Over the last two decades, four major scaffolding approaches for tissue engineering have evolved: pre-made porous scaffold, decellularized ECM, cell sheet with secreted ECM, cells encapsulated in self-assembled hydrogels [56,63].

Decellularized tissues have shown promising results in both preclinical and clinical applications. Allogenic tissues obtained from human cadavers represent ideal sources for scaffold development thanks to the higher similarity in the histomorphology and biomolecular composition with limited immunogenic reaction induced after appropriate decellularization [35].

Xenogeneic samples require additional treatment to remove alpha-gal epitopes on the graft, typical of non-old-World-monkeys and non-humans tissues [64,65].

Scaffolds derived from human skeletal muscles have been previously developed [49]. They demonstrated to improve muscle regeneration alone or in association with stem cells [6,13].

However, only limited studies dealing with human diaphragmatic muscle decellularization process are available in the literature with a paucity of detailed descriptions of microscopic, mechanical and biocompatibility characteristics [36-42,44,66-68].

Detergent-enzymatic decellularization processes have been applied successfully to human and non-human derived tissues. Depending on different tissue

to be treated, different combination of physical, enzymatic, and chemical treatments can be used. Ideally, researchers should aim to develop the mildest protocol to obtain acellular material without disruption of the structural and functional component of the ECM [69].

The assessment of appropriate removal of immunogenic elements with the preservation of muscle-specific ECM is a fundamental step to evaluate the efficacy of the decellularization process [70].

The project, aimed to define the best detergent-enzymatic protocol for the decellularization of human diaphragmatic patches, compared four different combinations of detergent-enzymatic processes modifying a previous successful protocol [49]. Triton X-100, the detergent previously used, has been recently considered cytotoxic to endocrine system and it is not usable for the development of human implantable devices.

Detergents are used in decellularization protocols to solubilize cell membranes and break protein/DNA relations. Non-ionic detergents (e.g. Tergitol^{TM}) are used to disrupt DNA-protein/lipid-lipid/lipid-protein interactions while ionic detergents cause cell solubilization through protein denaturation (e.g. SDS, SDC) [57,71].

In this study, both types and a combination of them (SDS+ Tergitol^{TM}) were used to substitute Triton X-100 after tissue immersion in deionized water and enzymatic treatment with DNase-I, trypsin and EDTA [72].

DNase-I allowed the interruption of nucleic acid sequences. Trypsin, in combination with EDTA, allowed the cleavage of cell-cell/cell-ECM adhesion limiting the damage to ECM proteins [73].

All protocols were completed in 6 days, limiting the overall time required for scaffold preparation.

Macroscopically the reduced intensity of the colors of treated muscle patches compared with native tissue can be explained by the disruption of muscle fibers.

Histological sections showed effective nuclei, cells (including muscle fibers) and DNA removal with all four protocols reducing significantly the immunogenic potential of the graft according to the literature [40,74]. Correspondingly, the absence of HLA-DR receptors confirms the low immunogenic potentials of decellularized grafts [37,67].

On the other hand, the presence and location of Collagen I and Laminin were preserved after all detergent-enzymatic protocols. Thus, ECM organization fundamental for cell adhesion, proliferation and migration appeared to be preserved after each treatment [75,76]. The disruption of the collagen network can change the mechanical behavior of the scaffold, affecting its the load bearing capacity and mechanical signals the are exposed to. In addition, a significant destruction of ECM components favors an enzymatic digestion of the scaffold in vivo with further degradation[27].

The quantification of GAGs component has been used as a parameter of preservation of original ECM structure, given the roles of these molecules in promoting muscle cell differentiation. In fact, removal of adhesive proteins and GAGs from the scaffold could impair cell migration and the bioactivity of the scaffold itself.

All protocol showed a satisfactory preservation of GAGs without significant differences. The higher preservation after Protocol n. 4 can be explained by high sensitivity of GAGs to ionic detergent used in Protocol n. 1,2,3 [70].

SHG imaging has been used to compare collagen quantification and organization between treated and native samples. The similar intensity of signals from SHG imaging confirmed the preservation of collagen fibers previously quantified with morphometric analysis. On the contrary, alternative decellularization protocol showed higher disruption of collagen fibers [77-79]. However, only Protocol n. 2 allowed a significant preservation the orientation of collagen fibers probably thanks to the combination of ionic and non-ionic detergents.

In addition to visualization of structural preservation of 3-D structure, the strain-stress response allowed a direct evaluation of mechanical properties of native and treated tissue samples.

The loss of anisotropy in decellularized samples, with similar response after longitudinal and transverse application of strain can be related with the alteration of collagen fibers orientation revealed with SHG imaging. Each different protocol impacted tissue stiffness differently. The reduction of stiffness measured in samples treated with Protocol n. 1, 2, 3 could be related to a slight reduction of collagen I fibers.

On the contrary, the increase of stiffness evident after the treatment with Protocol n. 4 appears to be related to the alteration of macroscopic aspect of muscle patches. Tergitol^{TM} alone could determine a disruption of normal collagen crimping with compactness reduction.

An essential phase to allow translational application from the basic research to the clinical setting is the confirmation of the safety of bio-engineered scaffolds.

Ad-MSCs have been shown to support muscle repair reducing scaffold reabsorption and scarring. Their capacity to differentiate into tissues of mesodermal lineage, together with their abundance and easiness to harvest make them promising cells in tissue engineering [13,80,81].

For these reasons, Ad-MSCs were chosen to plan future cell seeding and to evaluate scaffold cytotoxicity in this study. The indirect co-culture test, which can be considered as an indirect indication of adequate removal of toxic detergent, enzymes and reagents used, excluded any significant cytotoxic effect of treated diaphragm samples. Additionally, the presence of proliferating monolayers of seeded cells over muscle scaffold after each protocol confirmed the preservation of structural and molecular component of ECM required for cell adhesion and proliferation.

In vivo implantation of improperly decellularized scaffold can cause severe immunologic response with formation of seroma, abscess and graft rejection or

reabsorption. In addition, host reaction can be triggered by the persistence of toxic molecules used by the decellularization process itself [82].

Protocol n. 2 based on the association of both ionic and non-ionic detergents showed a favorable in vivo compatibility of the scaffold (because of the higher preservation of collagen fibers orientation collected with SHG).

The presence of a moderate lympho-monocytic infiltrate at the contact surface between the scaffold and the host displayed two weeks after implantation is compatible with the physiologic formation of a soft capsule around a foreign body. No massive infiltration of monocytes and microphages or signs of graft degradation were recognized [83-85].

The presence of VEGF-positive cells seems to be related to an early angiogenic process stimulated by the graft. On the contrary, the absence of myogenic process could explain the lack of myosin expression.

The results support further study evaluating the integration of the scaffold with its innervation/vascularization and Ad-MSC in vivo seeding [6,66].

One of the limits of our project for the creation of a scaffold aimed in the treatment of VML is the muscle chosen. In fact, due to the anatomy of the diaphragm muscle only relative thin muscles of the trunk (i.e. abdominal wall, back or diaphragm) could be regenerated with the implantation of the diaphragm muscle. Other strategies are needed for muscle regeneration in the extremities. The use of small patches applied as muscle graft instead of the use of the entire muscle as a scaffold have been proposed for muscle regeneration [49]. Alternatively, different muscles such as gracilis or latissimus dorsi muscles could be decellularized in their entirety.

In addition, the lack of vascularization of a scaffold, particularly in the presence of severely scarred recipient tissue, might reduce the chance of success of graft take increasing the risk of fibrosis, failure or complication, in particular when Ad-MSC are implanted at the same time. The lack of innervation could limit the

functional regeneration of the muscle. One of the vascular pedicles and the primary innervation of the diaphragm muscle could be harvested and decellularize to improve implantation in vivo.

CONCLUSIONS

The ideal scaffold derived from human cadaveric muscle still needs to be developed. Our project showed that human diaphragm is a valid source of muscle scaffold, which can be efficiently decellularized with detergent-enzymatic decellularization protocols using ionic and non-ionic detergents. All four protocols evaluated were able to remove immunogenic molecules maintaining biological activity, mechanical integrity and 3D structure of the native tissue. Protocol n. 2 based on the combination of SDS and Tergitol^{TM} was associated with the utmost preservation of collagen amount and orientation. No toxicity was reported both in vitro and in vivo.

Further studies based on animal model of VML injury should be performed to evaluate both tissue integration and functional performance of the scaffolds. In addition, in vivo cell seeding with Ad-MSC will allow to study the ability of muscle graft to stimulate cell differentiation towards muscle fibers.

REFERENCES

1. Knobloch K, Vogt PM. The reconstructive clockwork of the twenty-first century: an extension of the concept of the reconstructive ladder and reconstructive elevator. Plastic and reconstructive surgery. Oct 2010;126(4):220e-222e.
2. Kagaya Y, Arikawa M, Higashino T, Miyamoto S. Autologous abdominal wall reconstruction using anterolateral thigh and iliotibial tract flap after extensive tumor resection: A case series study of 50 consecutive cases. Journal of plastic, reconstructive & aesthetic surgery : JPRAS. Apr 2020;73(4):638-650.
3. Garvey PB, Martinez RA, Baumann DP, Liu J, Butler CE. Outcomes of abdominal wall reconstruction with acellular dermal matrix are not affected by wound contamination. Journal of the American College of Surgeons. Nov 2014;219(5):853-864.
4. Patel NG, Ratanshi I, Buchel EW. The Best of Abdominal Wall Reconstruction. Plastic and reconstructive surgery. Jan 2018;141(1):113e-136e.
5. Grasman JM, Zayas MJ, Page RL, Pins GD. Biomimetic scaffolds for regeneration of volumetric muscle loss in skeletal muscle injuries. Acta biomaterialia. Oct 2015;25:2-15.
6. Carnes ME, Pins GD. Skeletal Muscle Tissue Engineering: Biomaterials-Based Strategies for the Treatment of Volumetric Muscle Loss. Bioengineering (Basel, Switzerland). Jul 31 2020;7(3).
7. Grogan BF, Hsu JR. Volumetric muscle loss. The Journal of the American Academy of Orthopaedic Surgeons. 2011;19 Suppl 1:S35-37.
8. Pollot BE, Corona BT. Volumetric Muscle Loss. Methods in molecular biology (Clifton, N.J.). 2016;1460:19-31.
9. Greising SM, Corona BT, McGann C, Frankum JK, Warren GL. Therapeutic Approaches for Volumetric Muscle Loss Injury: A Systematic Review and Meta-Analysis. Tissue engineering. Part B, Reviews. Dec 2019;25(6):510-525.
10. Karalaki M, Fili S, Philippou A, Koutsilieris M. Muscle regeneration: cellular and molecular events. In vivo (Athens, Greece). Sep-Oct 2009;23(5):779-796.
11. Quarta M, Cromie M, Chacon R, et al. Bioengineered constructs combined with exercise enhance stem cell-mediated treatment of volumetric muscle loss. Nature communications. Jun 20 2017;8:15613.
12. Corona BT, Rivera JC, Owens JG, Wenke JC, Rathbone CR. Volumetric muscle loss leads to permanent disability following extremity trauma. Journal of rehabilitation research and development. 2015;52(7):785-792.
13. Olson LC, Redden JT, Gilliam L, et al. Human Adipose-Derived Stromal Cells Delivered on Decellularized Muscle Improve Muscle Regeneration and Regulate RAGE and P38 MAPK. Bioengineering (Basel, Switzerland). Aug 30 2022;9(9).
14. Garg K, Ward CL, Hurtgen BJ, et al. Volumetric muscle loss: persistent functional deficits beyond frank loss of tissue. Journal of orthopaedic research : official publication of the Orthopaedic Research Society. Jan 2015;33(1):40-46.
15. Lin CH, Lin YT, Yeh JT, Chen CT. Free functioning muscle transfer for lower extremity posttraumatic composite structure and functional defect. Plastic and reconstructive surgery. Jun 2007;119(7):2118-2126.
16. Liu J, Saul D, Böker KO, Ernst J, Lehman W, Schilling AF. Current Methods for Skeletal Muscle Tissue Repair and Regeneration. BioMed research international. 2018;2018:1984879.

17. Fischer JP, Elliott RM, Kozin SH, Levin LS. Free function muscle transfers for upper extremity reconstruction: a review of indications, techniques, and outcomes. The Journal of hand surgery. Dec 2013;38(12):2485-2490.
18. Tu YK, Yen CY, Ma CH, et al. Soft-tissue injury management and flap reconstruction for mangled lower extremities. Injury. Oct 2008;39 Suppl 4:75-95.
19. Houdek MT, Wellings EP, Mallett KE, Honig RL, Rose PS, Moran SL. Free Functional Latissimus Dorsi Reconstruction of the Quadriceps and Hamstrings following Oncologic Resection of Soft Tissue Sarcomas of the Thigh. Sarcoma. 2021;2021:8480737.
20. Borschel GH, Dow DE, Dennis RG, Brown DL. Tissue-engineered axially vascularized contractile skeletal muscle. Plastic and reconstructive surgery. Jun 2006;117(7):2235-2242.
21. Huang YC, Dennis RG, Larkin L, Baar K. Rapid formation of functional muscle in vitro using fibrin gels. Journal of applied physiology (Bethesda, Md. : 1985). Feb 2005;98(2):706-713.
22. Sicari BM, Dearth CL, Badylak SF. Tissue engineering and regenerative medicine approaches to enhance the functional response to skeletal muscle injury. Anatomical record (Hoboken, N.J. : 2007). Jan 2014;297(1):51-64.
23. Urciuolo A, De Coppi P. Decellularized Tissue for Muscle Regeneration. International journal of molecular sciences. Aug 14 2018;19(8).
24. Turner NJ, Badylak SF. Regeneration of skeletal muscle. Cell and tissue research. Mar 2012;347(3):759-774.
25. Carlson EC, Carlson BM. A method for preparing skeletal muscle fiber basal laminae. The Anatomical record. Jul 1991;230(3):325-331.
26. Lu H, Hoshiba T, Kawazoe N, Chen G. Comparison of decellularization techniques for preparation of extracellular matrix scaffolds derived from three-dimensional cell culture. Journal of biomedical materials research. Part A. Sep 2012;100(9):2507-2516.
27. Gilbert TW, Sellaro TL, Badylak SF. Decellularization of tissues and organs. Biomaterials. Jul 2006;27(19):3675-3683.
28. Greising SM, Rivera JC, Goldman SM, Watts A, Aguilar CA, Corona BT. Unwavering Pathobiology of Volumetric Muscle Loss Injury. Scientific reports. Oct 13 2017;7(1):13179.
29. Pollot BE, Goldman SM, Wenke JC, Corona BT. Decellularized extracellular matrix repair of volumetric muscle loss injury impairs adjacent bone healing in a rat model of complex musculoskeletal trauma. The journal of trauma and acute care surgery. Nov 2016;81(5 Suppl 2 Proceedings of the 2015 Military Health System Research Symposium):S184-S190.
30. Sarrafian TL, Bodine SC, Murphy B, Grayson JK, Stover SM. Extracellular matrix scaffolds for treatment of large volume muscle injuries: A review. Veterinary surgery : VS. May 2018;47(4):524-535.
31. Sicari BM, Rubin JP, Dearth CL, et al. An acellular biologic scaffold promotes skeletal muscle formation in mice and humans with volumetric muscle loss. Science translational medicine. Apr 30 2014;6(234):234ra258.
32. Badylak SF. Decellularized allogeneic and xenogeneic tissue as a bioscaffold for regenerative medicine: factors that influence the host response. Annals of biomedical engineering. Jul 2014;42(7):1517-1527.
33. Calve S, Simon HG. Biochemical and mechanical environment cooperatively regulate skeletal muscle regeneration. FASEB journal : official publication of the Federation of American Societies for Experimental Biology. Jun 2012;26(6):2538-2545.
34. McClure MJ, Cohen DJ, Ramey AN, et al. Decellularized Muscle Supports New Muscle Fibers and Improves Function Following Volumetric Injury. Tissue engineering. Part A. Aug 2018;24(15-16):1228-1241.

35. Porzionato A, Stocco E, Barbon S, Grandi F, Macchi V, De Caro R. Tissue-Engineered Grafts from Human Decellularized Extracellular Matrices: A Systematic Review and Future Perspectives. International journal of molecular sciences. Dec 18 2018;19(12).
36. Boso D, Carraro E, Maghin E, et al. Porcine Decellularized Diaphragm Hydrogel: A New Option for Skeletal Muscle Malformations. Biomedicines. Jun 22 2021;9(7).
37. Gubareva EA, Sjöqvist S, Gilevich IV, et al. Orthotopic transplantation of a tissue engineered diaphragm in rats. Biomaterials. Jan 2016;77:320-335.
38. Liao GP, Choi Y, Vojnits K, et al. Tissue Engineering to Repair Diaphragmatic Defect in a Rat Model. Stem cells international. 2017;2017:1764523.
39. Piccoli M, Urbani L, Alvarez-Fallas ME, et al. Improvement of diaphragmatic performance through orthotopic application of decellularized extracellular matrix patch. Biomaterials. Jan 2016;74:245-255.
40. Trevisan C, Fallas MEA, Maghin E, et al. Generation of a Functioning and Self-Renewing Diaphragmatic Muscle Construct. Stem cells translational medicine. Aug 2019;8(8):858-869.
41. Trevisan C, Maghin E, Dedja A, et al. Allogenic tissue-specific decellularized scaffolds promote long-term muscle innervation and functional recovery in a surgical diaphragmatic hernia model. Acta biomaterialia. Apr 15 2019;89:115-125.
42. Cozad MJ, Bachman SL, Grant SA. Assessment of decellularized porcine diaphragm conjugated with gold nanomaterials as a tissue scaffold for wound healing. Journal of biomedical materials research. Part A. Dec 1 2011;99(3):426-434.
43. Gamba PG, Conconi MT, Lo Piccolo R, Zara G, Spinazzi R, Parnigotto PP. Experimental abdominal wall defect repaired with acellular matrix. Pediatric surgery international. Sep 2002;18(5-6):327-331.
44. Davari HR, Rahim MB, Tanideh N, et al. Partial replacement of left hemidiaphragm in dogs by either cryopreserved or decellularized heterograft patch. Interactive cardiovascular and thoracic surgery. Oct 2016;23(4):623-629.
45. Barbon S, Stocco E, Contran M, et al. Preclinical Development of Bioengineered Allografts Derived from Decellularized Human Diaphragm. Biomedicines. Mar 22 2022;10(4).
46. Riederer BM, Bolt S, Brenner E, et al. The legal and ethical framework governing Body Donation in Europe ,?? 1st update on current practice. Eur. J. Anat. 2012;16:1-21.
47. De Caro R, Macchi V, Porzionato A. Promotion of body donation and use of cadavers in anatomical education at the University of Padova. Anatomical sciences education. Mar-Apr 2009;2(2):91-92.
48. Guidolin D, Porzionato A, Tortorella C, Macchi V, De Caro R. Fractal analysis of the structural complexity of the connective tissue in human carotid bodies. Frontiers in physiology. 2014;5:432.
49. Porzionato A, Sfriso MM, Pontini A, et al. Decellularized Human Skeletal Muscle as Biologic Scaffold for Reconstructive Surgery. International journal of molecular sciences. Jul 1 2015;16(7):14808-14831.
50. Schneider CA, Rasband WS, Eliceiri KW. NIH Image to ImageJ: 25 years of image analysis. Nature methods. Jul 2012;9(7):671-675.
51. Borile G, Sandrin D, Filippi A, Anderson KI, Romanato F. Label-Free Multiphoton Microscopy: Much More Than Fancy Images. International journal of molecular sciences. Mar 6 2021;22(5).
52. Filippi A, Dal Sasso E, Iop L, et al. Multimodal label-free ex vivo imaging using a dual-wavelength microscope with axial chromatic aberration compensation. Journal of biomedical optics. Mar 2018;23(9):1-9.

53. Schindelin J, Arganda-Carreras I, Frise E, et al. Fiji: an open-source platform for biological-image analysis. Nature methods. Jun 28 2012;9(7):676-682.
54. Wu S, Li H, Yang H, Zhang X, Li Z, Xu S. Quantitative analysis on collagen morphology in aging skin based on multiphoton microscopy. Journal of biomedical optics. Apr 2011;16(4):040502.
55. Todros S, Spadoni S, Maghin E, Piccoli M, Pavan PG. A Novel Bioreactor for the Mechanical Stimulation of Clinically Relevant Scaffolds for Muscle Tissue Engineering Purposes. Processes. 2021;9(3):474.
56. Schneider KH, Enayati M, Grasl C, et al. Acellular vascular matrix grafts from human placenta chorion: Impact of ECM preservation on graft characteristics, protein composition and in vivo performance. Biomaterials. Sep 2018;177:14-26.
57. Crapo PM, Gilbert TW, Badylak SF. An overview of tissue and whole organ decellularization processes. Biomaterials. Apr 2011;32(12):3233-3243.
58. Hwang W, Kelly NG, Boriek AM. Passive mechanics of muscle tendinous junction of canine diaphragm. Journal of applied physiology (Bethesda, Md. : 1985). Apr 2005;98(4):1328-1333.
59. Almouemen N, Kelly HM, O'Leary C. Tissue Engineering: Understanding the Role of Biomaterials and Biophysical Forces on Cell Functionality Through Computational and Structural Biotechnology Analytical Methods. Computational and structural biotechnology journal. 2019;17:591-598.
60. Bissell DM, Choun MO. The role of extracellular matrix in normal liver. Scandinavian journal of gastroenterology. Supplement. 1988;151:1-7.
61. Karp JM, Langer R. Development and therapeutic applications of advanced biomaterials. Current opinion in biotechnology. Oct 2007;18(5):454-459.
62. Schönherr E, Hausser HJ. Extracellular matrix and cytokines: a functional unit. Developmental immunology. 2000;7(2-4):89-101.
63. Chan BP, Leong KW. Scaffolding in tissue engineering: general approaches and tissue-specific considerations. European spine journal : official publication of the European Spine Society, the European Spinal Deformity Society, and the European Section of the Cervical Spine Research Society. Dec 2008;17 Suppl 4(Suppl 4):467-479.
64. Huai G, Qi P, Yang H, Wang Y. Characteristics of α-Gal epitope, anti-Gal antibody, α1,3 galactosyltransferase and its clinical exploitation (Review). International journal of molecular medicine. Jan 2016;37(1):11-20.
65. Tanemura M, Yin D, Chong AS, Galili U. Differential immune responses to alpha-gal epitopes on xenografts and allografts: implications for accommodation in xenotransplantation. The Journal of clinical investigation. Feb 2000;105(3):301-310.
66. Alvarèz Fallas ME, Piccoli M, Franzin C, et al. Decellularized Diaphragmatic Muscle Drives a Constructive Angiogenic Response In Vivo. International journal of molecular sciences. Apr 28 2018;19(5).
67. Conconi MT, Bellini S, Teoli D, et al. In vitro and in vivo evaluation of acellular diaphragmatic matrices seeded with muscle precursors cells and coated with VEGF silica gels to repair muscle defect of the diaphragm. Journal of biomedical materials research. Part A. May 2009;89(2):304-316.
68. Vellachi R, Kumar N, Saxena S, et al. Mesenchymal stem cell tailored bioengineered scaffolds derived from bubaline diaphragm and aortic matrices for reconstruction of abdominal wall defects. Journal of tissue engineering and regenerative medicine. Dec 2020;14(12):1763-1778.
69. Gillies AR, Smith LR, Lieber RL, Varghese S. Method for decellularizing skeletal muscle without detergents or proteolytic enzymes. Tissue engineering. Part C, Methods. Apr 2011;17(4):383-389.

70. White LJ, Taylor AJ, Faulk DM, et al. The impact of detergents on the tissue decellularization process: A ToF-SIMS study. Acta biomaterialia. Mar 1 2017;50:207-219.
71. Keane TJ, Swinehart IT, Badylak SF. Methods of tissue decellularization used for preparation of biologic scaffolds and in vivo relevance. Methods (San Diego, Calif.). Aug 2015;84:25-34.
72. Kim YS, Majid M, Melchiorri AJ, Mikos AG. Applications of decellularized extracellular matrix in bone and cartilage tissue engineering. Bioengineering & translational medicine. Jan 2019;4(1):83-95.
73. Das P, Singh YP, Mandal BB, Nandi SK. Tissue-derived decellularized extracellular matrices toward cartilage repair and regeneration. Methods in cell biology. 2020;157:185-221.
74. Sesli M, Akbay E, Onur MA. Decellularization of rat adipose tissue, diaphragm, and heart: a comparison of two decellularization methods. Turkish journal of biology = Turk biyoloji dergisi. 2018;42(6):537-547.
75. Csapo R, Gumpenberger M, Wessner B. Skeletal Muscle Extracellular Matrix - What Do We Know About Its Composition, Regulation, and Physiological Roles? A Narrative Review. Frontiers in physiology. 2020;11:253.
76. Xing Q, Parvizi M, Lopera Higuita M, Griffiths LG. Basement membrane proteins modulate cell migration on bovine pericardium extracellular matrix scaffold. Scientific reports. Feb 25 2021;11(1):4607.
77. Faulk DM, Carruthers CA, Warner HJ, et al. The effect of detergents on the basement membrane complex of a biologic scaffold material. Acta biomaterialia. Jan 2014;10(1):183-193.
78. Hwang J, San BH, Turner NJ, et al. Molecular assessment of collagen denaturation in decellularized tissues using a collagen hybridizing peptide. Acta biomaterialia. Apr 15 2017;53:268-278.
79. Merna N, Robertson C, La A, George SC. Optical imaging predicts mechanical properties during decellularization of cardiac tissue. Tissue engineering. Part C, Methods. Oct 2013;19(10):802-809.
80. Huang H, Liu J, Hao H, et al. Preferred M2 Polarization by ASC-Based Hydrogel Accelerated Angiogenesis and Myogenesis in Volumetric Muscle Loss Rats. Stem cells international. 2017;2017:2896874.
81. Pantelic MN, Larkin LM. Stem Cells for Skeletal Muscle Tissue Engineering. Tissue engineering. Part B, Reviews. Oct 2018;24(5):373-391.
82. Sotnichenko AS, Nakokhov RZ, Gubareva EA, Kuevda EV, Gumenyuk IS. Morphological Evaluation of the Tissue Reaction to Subcutaneous Implantation of Decellularized Matrices. Bulletin of experimental biology and medicine. Dec 2018;166(2):287-292.
83. Anderson JM, McNally AK. Biocompatibility of implants: lymphocyte/macrophage interactions. Seminars in immunopathology. May 2011;33(3):221-233.
84. Frazão LP, Vieira de Castro J, Neves NM. In Vivo Evaluation of the Biocompatibility of Biomaterial Device. Advances in experimental medicine and biology. 2020;1250:109-124.
85. Rodriguez A, Voskerician G, Meyerson H, MacEwan SR, Anderson JM. T cell subset distributions following primary and secondary implantation at subcutaneous biomaterial implant sites. Journal of biomedical materials research. Part A. May 2008;85(2):556-565.

RINGRAZIAMENTI

A Laura e Sofia che sono la gioia di ogni giorno.
A Silvia, Elena, Martina, ai Professori di Anatomia Umana e a LIFELAB per aver reso possibile questo progetto.
Al Prof. Bassetto e al Prof. Vindigni per le opportunità datemi nel corso di questi anni.